GRU
(Geodynamical Rheology Upscaling)

C. Thieulot & F. Gueydan

March 14, 2024

1 Mass and momentum conservation equations

we start from the mass and momentum conservation equations. Since our domain is very small gravitational forces are neglected.

$$\vec{\nabla}\cdot\boldsymbol{\sigma}+\rho\vec{g} = \vec{0} \quad (1)$$
$$\vec{\nabla}\cdot\vec{\mathrm{v}} = 0 \quad (2)$$

The full stress tensor is given by

$$\boldsymbol{\sigma}=-p\mathbf{1}+\boldsymbol{\tau}$$

where $\mathbf{1}$ is the unit matrix, p is the pressure and $\boldsymbol{\tau}$ is the deviatoric stress tensor which can be written as

$$\boldsymbol{\tau}=2\eta\dot{\boldsymbol{\varepsilon}}(\vec{\mathrm{v}})$$

where η is the viscosity, $\vec{\mathrm{v}}=(u,v)$ is the velocity vector, and $\dot{\boldsymbol{\varepsilon}}(\vec{\mathrm{v}})$ is the (deviatoric) strain rate tensor (we assume incompressible flow).

Putting it all together we obtain:

$$-\vec{\nabla}p+\vec{\nabla}\cdot(2\eta\dot{\boldsymbol{\varepsilon}}(\vec{\mathrm{v}}))+\rho\vec{g} = \vec{0} \quad (3)$$
$$\vec{\nabla}\cdot\vec{\mathrm{v}} = 0 \quad (4)$$

In what follows we assume the buoyancy forces are negligible, i.e. the term $\rho\vec{g}$ is neglected.

For the time being we assume the system is isothermal so the energy equation is not solved.

2 Numerical methods

The mass and momentum conservation equations are solved by means of the FE method. $Q_2\times Q_1$ elements are used [3]. The domain is a rectangle of size $L_x\times L_y$ with the lower left corner at $(x,y)=(0,0)$. The mesh is composed of nelx×nely elements. Boundary conditions are as follows: $\mathrm{v}_y=0$ is prescribed on all boundaries, while $\mathrm{v}_x=\pm\mathrm{v}_0$ is prescribed at the top and at the bottom (of opposite sign) so that the background strain rate is given by

$$\dot{\varepsilon}_b=\frac{\mathrm{v}_0}{L_y}$$

Typically we set $L_y=1$ cm and $\dot{\varepsilon}_b=10^{-15}$ s^{-1} so that $\mathrm{v}_0=\dot{\varepsilon}_b L_y\simeq 3.2\cdot 10^{-8}$ cm/year. Calculations are performed until a strain value $\gamma=2$ has been reached, i.e. $t_{final}=\gamma/\dot{\varepsilon}_b\simeq 2\times 10^{15}$ s $\simeq 64$ Myr.

INSERT here fig of velocity is square

A cloud of passive markers (hereafter called swarm[1]) is place in the domain. The nmarker_per_dim parameter controls the number of markers placed in each element at the beginning of the simulation: nmarker_per_element=nmarker_per_dim**2 while the total number of markers in the domain is then nmarker=nel*nmarker_per_element. Markers are initially placed on a regular grid of positions inside each element, as shown in Fig.XX

INSERT here figure with markers at t=0

[1] https://en.wikipedia.org/wiki/Swarm_behaviour

Each marker carries a lot of information stored in the swarm_xxx arrays, where xxx stands for the name of the field, such as x,y,gs,eta,...

At each time step markers are localised (i.e. we find in which element they reside in, the (effective) strain rate is interpolated onto them and passed as argument to the viscosity function which, based on the temperature T and the grain size d of each marker computes the effective viscosity (see Section 3).

This viscosity is then averaged inside the element and is used to build the elemental matrix K_η. Note that the averaging can be arithmetic, geometric or harmonic (default).

The FE matrix is assembled using lil_matrix , converted to CSR format and then passed to a direct solver alongside the rhs vector. Node that the code is based on the codes available in the educational Fieldstone project [2] and is therefore not optimised for performance.

Following a standard approach, the discretised Stokes equations yield the following linear system

$$\begin{pmatrix} \mathbb{K} & \mathbb{G} \\ \mathbb{G}^T & 0 \end{pmatrix} \cdot \begin{pmatrix} \vec{\mathcal{V}} \\ \vec{\mathcal{P}} \end{pmatrix} = \begin{pmatrix} \vec{f} \\ \vec{h} \end{pmatrix}$$

where $\vec{\mathcal{V}}$ is the vector containing all velocity degrees of freedom (size NfemV=NV* ndofV) and $\vec{\mathcal{P}}$ is the vector containing all pressure degrees of freedom (size NfemP= NP* ndofP).

After the FE matrix has been built, the linear system is solved, and we have obtained a new velocity and pressure field.

We then proceed to compute the strain rate components on the nodes. Since a given node belongs to more than one element the nodal values are averages of the corner values of neighbouring elements. The nodal effective strain rate is then computed as follows:

$$\dot{\varepsilon}_e = \sqrt{\frac{1}{2}(\dot{\varepsilon}_{xx}^2 + \dot{\varepsilon}_{yy}^2) + \dot{\varepsilon}_{xy}^2)}$$

Because the effective viscosity of each marker (and therefore each element) depends on the strain rate, we carry out simple Picard nonlinear iterations which stop when the 2-norm of the relative change of the velocity field between two consecutive iterations is less than a set tolerance of 10^{-4}.

The nodal velocity is used to advect the markers. For simplicity we resort to an Euler step, i.e.

$$\vec{\mathrm{x}}_i(t+\delta t) = \vec{\mathrm{x}}_i(t) + \vec{\mathrm{v}}_i \; \delta t \qquad i = 1, ...nmarker$$

The timestep δt is controled by a CFL condition with $C = 0.25$:

$$\delta t = C \frac{h}{\max |\vec{\mathrm{v}}|_\Omega}$$

where h is the element size and $C \in [0, 1[$.

At the beginning each marker is assigned a grain size $d = 1000$ µm. In the middle of the domain random noise is added as shown in Fig.YYY

INSERT fig of initial d

It is a gaussian distribution with a prescribed standard deviation of 10% of the initial background grain size. The grain size value carried by each marker is evolved according the equation presented in Section 4.

3 Strain rate decomposition

The strain rate is to be decomposed into its various contributions coming from the different deformation mechanisms, dislocation creep, diffusion creep, disGBS and low-temperature plasticity:

$$\dot{\varepsilon} = \dot{\varepsilon}_{dsl} + \dot{\varepsilon}_{dif} + \dot{\varepsilon}_{gbs} + \dot{\varepsilon}_{exp}$$

with

$$\dot{\varepsilon}_{dsl} = A_{dsl} \exp\left(-\frac{Q_{dsl}}{RT}\right) \tau^{n_{dsl}} \tag{5}$$

$$\dot{\varepsilon}_{dif} = A_{dif} \exp\left(-\frac{Q_{dif}}{RT}\right) \tau^{n_{dif}} d^{-m_{dif}} \tag{6}$$

$$\dot{\varepsilon}_{gbs} = A_{gbs} \exp\left(-\frac{Q_{gbs}}{RT}\right) \tau^{n_{gbs}} d^{-m_{gbs}} \tag{7}$$

$$\dot{\varepsilon}_{exp} = A_{exp} \exp\left[-\frac{Q_{exp}}{RT}\left(1 - \frac{\tau}{\tau_p}\right)^{n_{exp}}\right] \tag{8}$$

[2] https://cedrict.github.io/

where d is the grain size, m is the grain size exponent, τ_p is the Peierls stress defined for low-temperature plasticity.

Note that the first 3 equations above can be re-written:

$$\tau = \left(\frac{\dot{\varepsilon}_{dsl}}{A_{dsl}}\right)^{1/n_{dsl}} \exp\left(\frac{Q_{dsl}}{n_{dsl}RT}\right) \tag{9}$$

$$\tau = \left(\frac{\dot{\varepsilon}_{dif}}{A_{dif}}\right)^{1/n_{dif}} \exp\left(\frac{Q_{dsl}}{n_{dif}RT}\right) d^{m_{dif}/n_{dif}} \tag{10}$$

$$\tau = \left(\frac{\dot{\varepsilon}_{gbs}}{A_{gbs}}\right)^{1/n_{gbs}} \exp\left(\frac{Q_{gbs}}{n_{gbs}RT}\right) d^{m_{gbs}/n_{gbs}} \tag{11}$$

$$\tag{12}$$

There is one major problem with the equations above: Assuming $\dot{\varepsilon}$ and temperature T known (as well as all the material parameters A, Q, n, ...), and that the deformation mechanisms are in series and subjected to the same deviatoric stress τ, we must find τ such that

$$\mathcal{F}(\tau) = \dot{\varepsilon} - \dot{\varepsilon}_{dsl}(\tau) - \dot{\varepsilon}_{dif}(\tau) - \dot{\varepsilon}_{gbs}(\tau) - \dot{\varepsilon}_{exp}(\tau) = 0$$

Unfortunately, this equation is non-linear in τ so that finding its zero(es) is not straightforward. A Newton-Raphson[3] algorithm is then used. How to build such an algorithm is presented in Section 2.27.22 of FieldStone but we will here use an existing python function. We load scipy.optimize module and use the newton function[4] which finds a zero of a real or complex function using the Newton-Raphson (or secant or Halley's) method. Once τ (tau_NR) has been found, it can then be inserted in the strain rate equations above and the strain rate partitioning is then complete.

4 Grain size evolution

Following Précigout and Gueydan [2], we simulate a dynamic grain size reduction by using the following grain size evolution law Braun et al. [1], that relates the rate of change of grain size $\dot{d}$ to the deformation rate $\dot{\varepsilon}$ according to

$$\dot{d} = -\frac{\dot{\varepsilon}}{\dot{\varepsilon}_T}(d - d_\infty)$$

where d_∞ can be defined in multiple ways:

- in Braun et al. [1], it obeys the following piezometric relationship

  $$d_\infty = B\tau^{-p}$$

  where d_∞ is the recrystallized grain size defined by the field boundary hypothesis

  As of now this option is not implemented.

- in Précigout and Gueydan [2] it is defined as the boundary between GBS and diff or disl and diff. In this paper d_∞ is the recrystallized grain size defined by the field boundary hypothesis and is shown on the following figure:

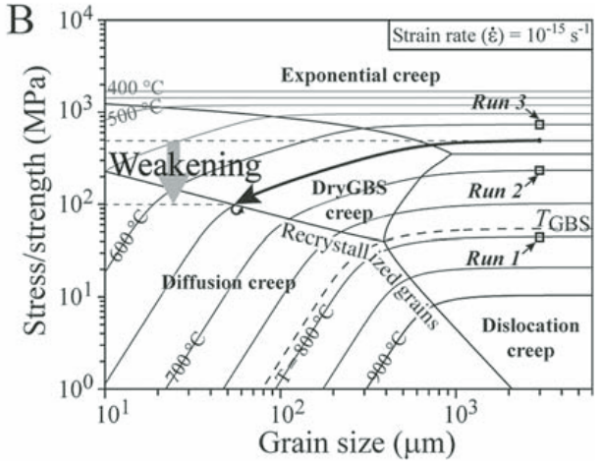

[3] https://en.wikipedia.org/wiki/Newton's_method

[4] https://docs.scipy.org/doc/scipy/reference/generated/scipy.optimize.newton.html

Let us first consider the GBS-diff boundary. Exactly on the line both mechanisms have the same strain rate (50% of the total strain rate) and same stress τ .

$$\tau = \left(\frac{\dot{\varepsilon}}{A_{dif}} \exp\left(\frac{Q_{dif}}{RT} \right) d^{m_{dif}} \right)^{1/n_{dif}} = \left(\frac{\dot{\varepsilon}}{A_{gbs}} \exp\left(\frac{Q_{gbs}}{RT} \right) d^{m_{gbs}} \right)^{1/n_{gbs}}$$

$$\left(\frac{\dot{\varepsilon}}{A_{dif}} \right)^{1/n_{dif}} \exp\left(\frac{Q_{dif}}{RTn_{dif}} \right) d^{m_{dif}/n_{dif}} = \left(\frac{\dot{\varepsilon}}{A_{gbs}} \right)^{1/n_{gbs}} \exp\left(\frac{Q_{gbs}}{n_{gbs}RT} \right) d^{m_{gbs}/n_{gbs}}$$

$$d^{m_{dif}/n_{dif}} d^{-m_{gbs}/n_{gbs}} = \left(\frac{\dot{\varepsilon}}{A_{gbs}} \right)^{1/n_{gbs}} \left(\frac{\dot{\varepsilon}}{A_{dif}} \right)^{-1/n_{dif}} \exp\left(\frac{Q_{gbs}}{n_{gbs}RT} \right) \exp\left(-\frac{Q_{dif}}{RTn_{dif}} \right)$$

$$d^{m_{dif}/n_{dif} - m_{gbs}/n_{gbs}} = \left(\frac{\dot{\varepsilon}}{A_{gbs}} \right)^{1/n_{gbs}} \left(\frac{\dot{\varepsilon}}{A_{dif}} \right)^{-1/n_{dif}} \exp\left(\frac{1}{RT} (\frac{Q_{gbs}}{n_{gbs}} - \frac{Q_{dif}}{n_{dif}}) \right)$$

$$d_\infty = \left[\left(\frac{\dot{\varepsilon}}{A_{gbs}} \right)^{1/n_{gbs}} \left(\frac{\dot{\varepsilon}}{A_{dif}} \right)^{-1/n_{dif}} \exp\left(\frac{1}{RT} (\frac{Q_{gbs}}{n_{gbs}} - \frac{Q_{dif}}{n_{dif}}) \right) \right]^{1/(m_{dif}/n_{dif} - m_{gbs}/n_{gbs})}$$

This expression is a function of temperature T and strainrate.

Likewise we can establis the grain size d_∞ at the boundary between dis and diff (note that dis does not depend on grain size so $m_{dis} = 0$:

$$d_\infty = \left[\left(\frac{\dot{\varepsilon}}{A_{dis}} \right)^{1/n_{dis}} \left(\frac{\dot{\varepsilon}}{A_{dif}} \right)^{-1/n_{dif}} \exp\left(\frac{1}{RT} (\frac{Q_{dis}}{n_{dis}} - \frac{Q_{dif}}{n_{dif}}) \right) \right]^{n_{dif}/m_{dif}}$$

This is all implemented in 3 functions: compute_dinf_gbs_diff, compute_dinf_dis_diff, compute_dinf. We have implemented a standalone code which computes d_∞ for a wide array of temperatures.

5 shear heating

For incompressible materials, and neglecting diffusion and advection processes, the energy equation is then

$$\rho C_p \frac{\partial T}{\partial t} = 2\eta \dot{\boldsymbol{\varepsilon}} : \dot{\boldsymbol{\varepsilon}}$$

or,

$$\frac{\partial T}{\partial t} = \frac{2\eta}{\rho C_p} (\dot{\varepsilon}_{xx}^2 + \dot{\varepsilon}_{yy}^2 + 2\dot{\varepsilon}_{xy}^2)$$

This means that we can write a simple post-processor that computes for each marker the maximum temperature generated by shear heating. Of course in the absence of diffusion this remains an upper bound only meant to provide us with a rough estimate.

References

[1] J. Braun et al. "A simple parameterization of strain localization in the ductile regime due to grain-size reduction: a case study for olivine". In: 104 (1999), pp. 25, 167–25, 181. DOI: 10.1029/1999JB900214.

[2] Jacques Précigout and Frédéric Gueydan. "Mantle weakening and strain localization: Implications for the long-term strength of the continental lithosphere". In: *Geology* 37.2 (2009), pp. 147–150. DOI: 10.1130/G25239A.1.

[3] C. Thieulot and W. Bangerth. "On the choice of finite element for applications in geodynamics". In: *Solid Earth* 13 (2022), pp. 229–249. DOI: 10.5194/se-13-1-2022.